The Prostate 47:118 – 124 (2001)

Transrectal Ultrasound for Monitoring Murine Orthotopic Prostate Tumor

Nobuyuki Kusaka,[1] Yasutomo Nasu,[1]* Ryoji Arata,[1] Takashi Saika,[1] Tomoyasu Tsushima,[1] Robert Kraaij,[2] Chris H. Bangma,[2] and Hiromi Kumon[1]

[1]Department of Urology, Okayama University Medical School, Okayama, Japan
[2]Department of Experimental Urology, Erasmus University, Rotterdam, The Netherlands

BACKGROUND. The mouse orthotopic prostate tumor model has been recognized as an ideal preclinical animal model simulating the anatomical and biological milieu of the prostate. In comparison with the subcutaneous tumor model, the only disadvantage of this model is the difficulty of chronological tumor growth monitoring. We have applied recent endoluminal ultrasound technology, transrectal ultrasonography (TRUS), to the monitoring of mouse orthotopic prostate tumors.

METHODS. A 6 Fr. 20 MHz catheter-based radial scan probe was used and TRUS was performed without any prior preparation including anesthesia. Orthotopic tumors were initiated by inoculation of 5000 RM-9 cells into the dorsal prostate of 12-week-old C57BL/6 male mice. The tumor growth was monitored by TRUS from day 3 to day 21. In addition, TRUS was performed to detect tumor growth suppression after intraperitoneal administration of *cis*-diamminedichloroplatinum (CDDP).

RESULTS. By ultrasound, tumors became detectable 7 days after tumor cell inoculation. TRUS images were clear and parallel to actual tumor growth. The tumor volume (X) calculated by TRUS correlated significantly with the actual tumor weight (Y) measured at autopsy; $Y = 101.653 + 1.174X$ ($R = 0.930$, $P < 0.001$). Similarly, tumor growth suppression induced by CDDP was clearly detected by TRUS with reasonable accuracy.

CONCLUSIONS. A high resolution TRUS allows simple and reliable monitoring of in situ tumor growth and growth suppression, making the mouse orthotopic prostate tumor model more efficient. *Prostate 47:118–124, 2001.* © 2001 Wiley-Liss, Inc.

KEY WORDS: **prostate cancer; animal model; orthotopic implantation; ultrasonography**

INTRODUCTION

Although orthotopic implantation models offer the potential for improved modeling of tumor development and therapeutic response, noninvasive methods have not been readily available to monitor tumor growth serially at internal sites in small rodents. The mouse orthotopic prostate tumor model has been recognized as an ideal preclinical animal model simulating the anatomical and biological mileau of the prostate [1–8]. Many preclinical studies have been conducted using this model system [9–13]. In comparison with the subcutaneous (SC) tumor model, the single disadvantage of this model was the difficulty of chronological monitoring of tumor growth. Current assessment methods generally use caliper measurements of tumors growing at accessible SC sites or caliper measurement/tumor weight measurement made at autopsy or laparotomy [9]. Therefore, we believe that the development of an easily implemented noninvasive approach is necessary to monitor the longitudinal tumor growth at internal sites.

Recently, endoluminal ultrasound with a catheter-based probe (7.5–20 MHz) has been used clinically in

*Correspondence to: Yasutomo Nasu, MD, Department of Urology, Okayama University Medical School, 2-5-1 Shikata, Okayama 700-8558, Japan. E-mail ynasu@med.okayama-u.ac.jp

Received 11 September 2000; Accepted 27 December 2000

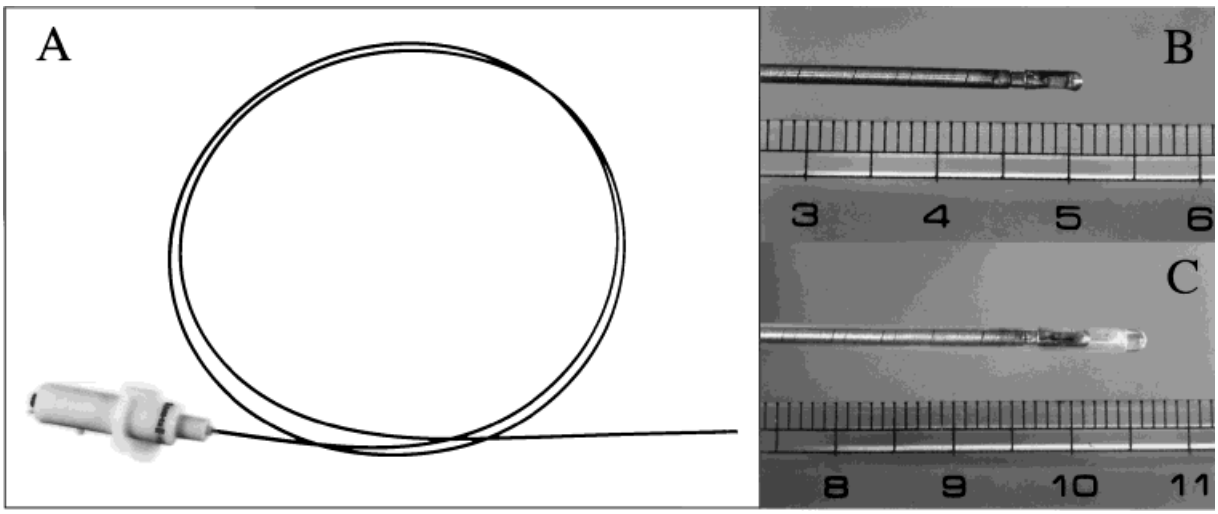

Fig. 1. An endoluminal ultrasound probe for TRUS. **A:** Whole appearance of a 20-MHz-based radial scan probe integrated into a 6 Fr. catheter. **B:** Tip of the transducer. **C:** Tip of the probe covered with an outer catheter filled with water.

detecting various pathological conditions of blood vessels, the esophagus, stomach, and ureters [14–17]. We applied this fine ultrasound probe to transrectal ultrasound (TRUS) for orthotopic mouse tumors and assessed the efficacy in monitoring not only tumor growth but also tumor growth suppression in the murine prostate.

MATERIALS AND METHODS

Animals

C57BL/6 male mice (10–12 weeks) were purchased from the Charles River Laboratories Inc. (Wilmington, MA). Experimental animals were housed and handled in accordance with Okayama University Animal Research Committee Guidelines.

Mouse Prostate Cancer Cell Line

The RM-9 mouse prostate cancer cell line was kindly provided by Dr. T. C. Thompson (Baylor College of Medicine, Houston). The cell line, RM-9, was derived from a primary prostate tumor induced in the Zipras/myc-9 infected mouse prostate reconstitution (MPR) model system using C57BL/6 mice [18]. Cells were maintained in the Dulbecco Modified Eagle Medium (DMEM; Nissui Pharmaceutical Co., Ltd. Tokyo, Japan) with 10% fetal bovine serum (FBS; Gibco BRL, Grand Island, NY), without the use of antibiotics.

Orthotopic Tumor Implantation

At orthotopic tumor inoculation, syngeneic C57BL/6 male mice were anesthetized with sodium pentobarbital (0.1 mg/g body weight, intraperitoneally), and placed in the supine position. A low abdominal transverse incision was made and the bilateral dorsal lobes of the prostate were exposed.

Following the trypsinization, 5×10^3 RM-9 cells in 10μl Hank buffered saline solution (HBSS) were injected using a 30-gage needle and a 25-μl glass syringe (Hamilton Co., Reno, NV) directly into the right dorsal lobe of the prostate under a dissecting microscope. A clearly recognizable bleb within the injected prostatic lobe was considered as the sign of a technically satisfactory injection. The abdominal wound was closed with stainless steel clips (Autoclip; Becton Dickinson and Co., Sparks, MD).

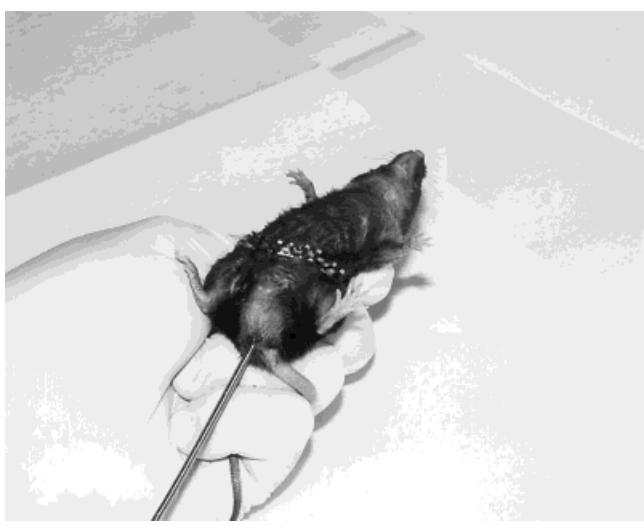

Fig. 2. Procedure for TRUS. A lubricated ultrasound probe is inserted into the rectum, while the mouse is held securely without anesthesia.

Transrectal Ultrasound Imaging

A 20-MHz-based radial scan probe integrated into a 6 Fr. catheter (ALOKA CO., LTD. Tokyo, Japan) and an ultrasound unit (SSD-550, ALOKA CO., LTD.) were used for this study (Fig. 1). The 20-MHz transducer provides high-resolution images with an axial resolution of 0.2 mm and revolves at 15 frames per second producing a 360° cross-sectional real time image.

The tip of the catheter was lubricated with ultrasound gel and inserted into the rectum while the mouse was secured without anesthesia (Fig. 2).

Measurement of the Orthotopic Tumor Growth

TRUS was conducted on days 3, 7, 10, 14, 17, and 21 after tumor cell inoculation. At the area of greatest transverse diameter in the axial plane, the anteroposterior and transverse dimensions of the tumor were measured and recorded. All observed images were printed out immediately. Each tumor volume was calculated according to the method of Janik et al. [19]: volume $= (m_1)^2 \times m_2 \times 0.5236$; m_1 represents the shorter axis and m_2 the longer axis. On days 7, 14, and 21, the mice were sacrificed following the ultrasonic measurement, the tumors were removed carefully, and the actual tumor weight (tumor wet weight) was measured.

A total of 80 mice was used to make up the number in each experimental group to be 25, based on our previous experience with 96% of average tumor take rate and 1–2% of anesthesia death. A mouse was excluded from the study if the tumor formation was not detected both at TRUS and macroscopic inspection at autopsy.

Detection of Tumor Growth Suppression

cis-diamminedichloroplatinum (CDDP) was used for the experiment to detect tumor growth suppression by TRUS. CDDP (Sigma Chemical Co., St. Louis, MO) was dissolved in 0.9% NaCl, and injected intraperitoneally at a dose of 125 mg/mouse on day 7 after tumor cell inoculation. Control mice were injected intraperitoneally with PBS. TRUS and subsequent measurement of actual tumor weight at

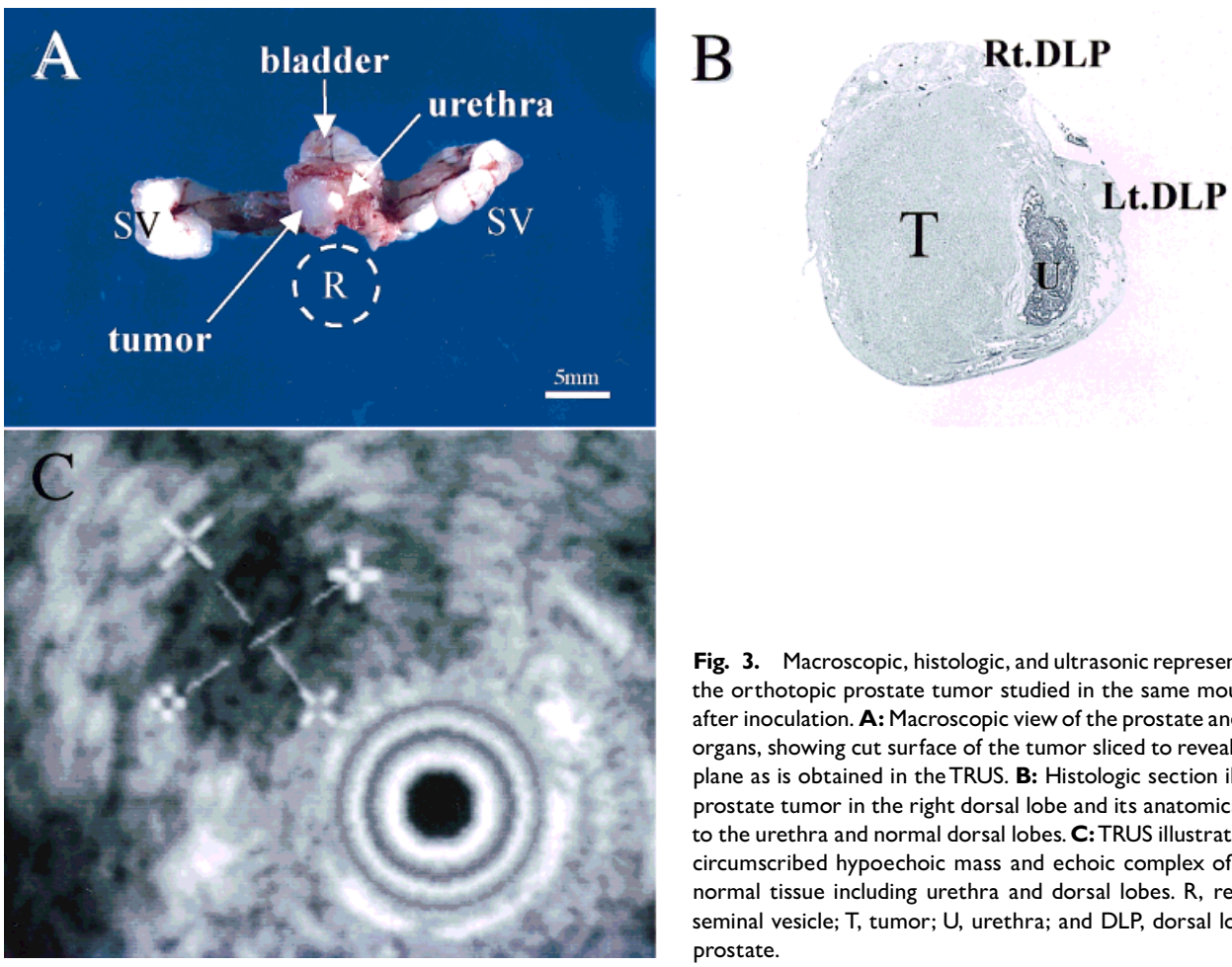

Fig. 3. Macroscopic, histologic, and ultrasonic representations of the orthotopic prostate tumor studied in the same mouse 7 days after inoculation. **A:** Macroscopic view of the prostate and adjacent organs, showing cut surface of the tumor sliced to reveal the same plane as is obtained in the TRUS. **B:** Histologic section illustrating prostate tumor in the right dorsal lobe and its anatomical relation to the urethra and normal dorsal lobes. **C:** TRUS illustrating a well-circumscribed hypoechoic mass and echoic complex of displaced normal tissue including urethra and dorsal lobes. R, rectum; SV, seminal vesicle; T, tumor; U, urethra; and DLP, dorsal lobe of the prostate.

autopsy were performed on days 14 and 21 using five mice for each group at each time point.

RESULTS

Orthotopic Tumor Imaging

When the probe was inserted about 1–2 cm into the rectum, the normal prostate gland (dorsal robe), urethra and peri-urethral tissue were observed. The bilateral testis, seminal vesicle, and bladder were also clearly recognized (data not shown). The bladder and urethra were good markers for detecting the prostate gland.

After tumor cell inoculation, the growth of orthotopic tumors was clearly depicted in the TRUS images from day 7 to day 21 (Figs. 3, 4). At day 3, no clear tumors were detected by TRUS. Our previous study indicates that a whitish protrusion (1–2 mm in diameter), which is compatible with microscopic tumor formation, is identified macroscopically at necropsy 3 days after orthotopic cell injection.

After 7 days, prostate tumors developing in the right dorsal lobe were detected unambiguously as small, hypoechoic masses adjacent to the urethra by TRUS (Fig. 3). The TRUS images of orthotopic tumors at this early stage coincided well with macroscopic and histologic findings as demonstrated in Figure 3. Since the tumors had grown to over 8–10 mm in diameter 14 days after inoculation, the subsequent ultrasonic measurements of hypoechoic, relatively homogeneous lesions on days 14, 17, and 21 after inoculation were easily conducted within a minute. As illustrated in Figure 4, the TRUS images of the tumors on days 14 and 21 coincided well with macroscopic views of cut surfaces of the tumors sliced in the same plane as in the TRUS. The mean time required to perform ultrasound measurement was less than 2 minutes ranged from 50 seconds (days 14, 21) to 1 minute and 40 seconds (day 7).

Tumor Volume Measurement

The relationship between tumor volume calculated by TRUS and the actual tumor weight (tumor wet weight) on days 7, 14, and 21 was analyzed. Among 80 mice injected, 3 mice died related to the anesthesia

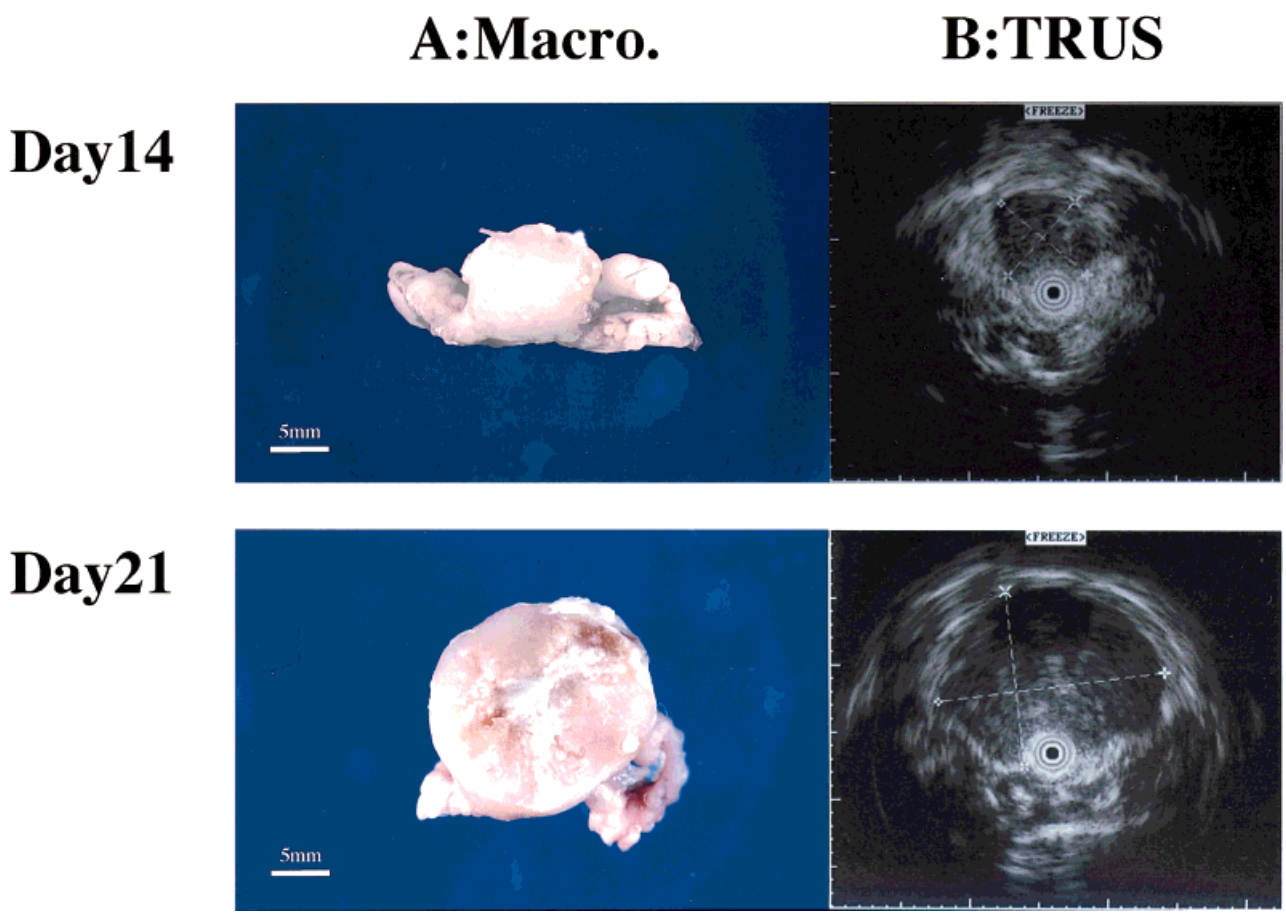

Fig. 4. Macroscopic and ultrasonic representations of the orthotopic prostate tumor in the same mouse studied on days 14 and 21, respectively. The extirpated tumors are sliced to reveal the same cut surface as observed by TRUS.

TABLE I. TRUS Measurement and Actual Measurement of Orthotopic Prostate Tumors on days 7, 14, and 21 (mean ± SE)

	TRUS measurement			Actual measurement
Day	Short axis (mm)	Long axis (mm)	Calculated volume (mm^3)	Weight (mg)
7 (n = 21)	3.89 ± 0.23	5.40 ± 0.35	47.90 ± 7.71	76.94 ± 9.37
14 (n = 25)	8.81 ± 0.17	11.61 ± 0.33	477.60 ± 22.96	697.91 ± 47.58
21 (n = 25)	11.48 ± 0.21	13.98 ± 0.36	979.70 ± 51.65	1235.21 ± 76.78

(death rate 3.75%). On day 7, 25 mice received TRUS, 24 mice of these had detectable tumors, but sufficient and adequate tumor specimens could not be obtained in 3 mice due to technical error. Finally, 21 mice were included in the study on day 7. On days 14 and 21, 26 mice received TRUS, respectively, and one mouse in each group did not form any tumor. Overall tumor take rate was 96.1% (74/77). Table I shows mean tumor size and volume calculated by TRUS and the actual tumor weight at autopsy at each time point. As demonstrated in Figure 5, the tumor volume calculated by TRUS (X) correlated significantly with the actual tumor weight (Y) measured at autopsy; $Y = 101.653 + 1.174X$ ($R = 0.930$, $P < 0.001$). Throughout the TRUS imaging without anesthesia, no adverse events like rectal perforation were experienced. And no evidence of hematoma formation, perforation or other injury to the rectum and colon was observed at the time of necropsy.

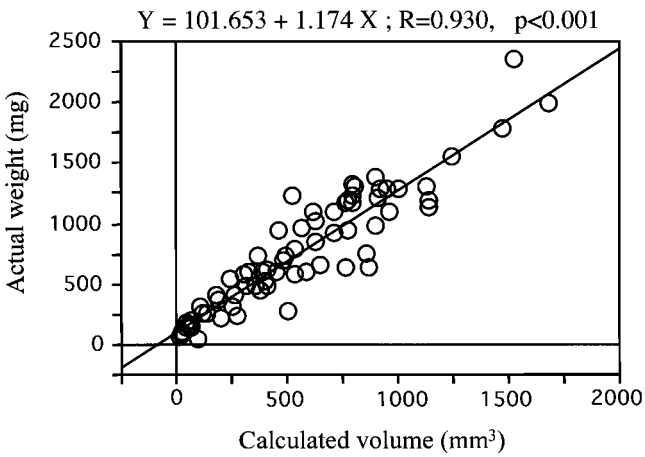

Fig. 5. Correlation between calculated tumor volume and actual tumor weight (n = 71) X axis, calculated volume; and Y axis, actual weight.

Detection of Tumor Growth Suppression

The tumor growth suppression induced by CDDP was also detected clearly by TRUS in the mouse orthotopic model. The decreased tumor volume observed by TRUS in the treatment group correlated well with the actual tumor measurement at autopsy on days 14 and 21 (Fig. 6).

DISCUSSION

The orthotopic mouse model of the prostate tumor is recognized as an indispensable animal model system for pre-clinical studies in the development of new therapies including gene therapy [10–12]. The applicability of this model will be further expanded when a reliable system is developed to monitor in situ tumor growth and growth suppression. Since such a monitoring system significantly decreases the number of experimental animals used by omitting the sacrifice of mice at each time point for evaluation, a more sophisticated and informative study may be carried out in a single experiment.

Recently, imaging technology including ultrasound and magnetic resonance imaging (MRI) has improved dramatically. Some investigators successfully used MRI to detect intravesical growth of murine bladder tumors, demonstrating accurate volumetric measurement and longitudinal monitoring [20,21]. Although MRI is undoubtedly noninvasive and can be applied repeatedly, it is expensive and relatively time-consuming. Similarly, several investigators reported noninvasive monitoring of tumor growth in animal models using ultrasound [22–25]. The occurrence and tumor growth in the rat liver were clearly observed by transabdominal ultrasound [22]. Alexander

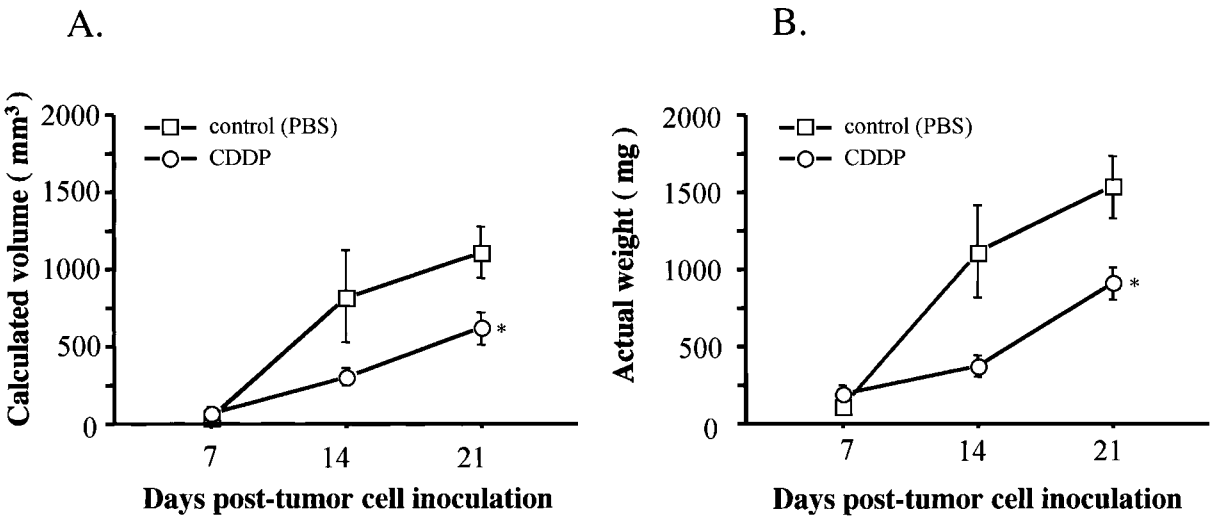

Fig. 6. CDDP-induced tumor growth suppression detected by TRUS (**A**) and actual tumor measurement (**B**). Results are expressed as mean ± SE (n = 5). CDDP treatment group vs. control group, $P < 0.05$, unpaired *t* test.

et al. [25] reported the usefulness of TRUS for monitoring of murine orthotopic bladder tumors. To our knowledge, however, concerning the orthotopic mouse model of prostate cancer, there has been no report on chronological ultrasonic monitoring of tumor growth.

In clinical practice, the TRUS system is generally used as a noninvasive, repeatable, and cost-effective examination to observe prostatic lesions. Over the last few years new small-caliber, high-frequency ultrasound equipment has been developed, refining the application and resolution of endoluminal ultrasound [14–17,26,27]. In the present TRUS study, we have used an endoluminal ultrasound transducer (size 6 F, 20 MHz), mainly for detection of minute ureteral lesions in humans. The use of TRUS requires minimal skill, and it is easy to observe mouse orthotopic prostate tumors accurately in a short period of time without anesthesia. In terms of technical simplicity, noninvasiveness, and cost-effectiveness, TRUS is far superior to MRI in the monitoring of murine orthotopic tumors.

Furthermore, the present study demonstrated that the tumor volume calculated by TRUS correlated significantly with the actual tumor weight measured at autopsy. TRUS also confirmed that not only tumor growth but also tumor growth suppression induced by anti-cancer drugs could be sufficiently monitored over a period of time. Based on the present results, we are planning to conduct several pre-clinical studies by using the mouse orthotopic prostate tumor model combined with TRUS monitoring. In these future studies, we will investigate the applicability of new technology including color Doppler to the evaluation of qualitative changes of the tumor during tumor growth and/or treatment response.

REFERENCES

1. An Z, Wang X, Geller J, Moossa AR, Hoffman RM. Surgical orthotopic implantation allows high lung and lymph node metastatic expression of human prostate carcinoma cell line PC-3 in nude mice. Prostate 1998;34:169–174.
2. Baley PA, Yoshida K, Qian W, Sehgal I, Thompson TC. Progression to androgen insensitivity in a novel in vitro mouse model for prostate cancer. J Steroid Biochem Mol Biol 1995;52:403–413.
3. Waters DJ, Janovitz EB, Chan TC. Spontaneous metastasis of PC-3 cells in athymic mice after implantation in orthotopic or ectopic microenvironments. Prostate 1995;26:227–234.
4. Rembrink K, Romijn JC, van der Kwast TH, Rübben H, Schröder FH. Orthotopic implantation of human prostate cancer cell lines: A clinically relevant animal model for metastatic prostate cancer. Prostate 1997;31:168–174.
5. Pettaway CA, Pathak S, Greene G, Ramirez E, Wilson MR, Killion JJ, Fidler IJ. Selection of highly metastatic variants of different human prostatic carcinomas using orthotopic implantation in nude mice. Clin Cancer Res 1996;2:1627–1636.
6. Vieweg J, Heston WD, Gilboa E, Fair WR. An experimental model simulating local recurrence and pelvic lymph node metastasis following orthotopic induction of prostate cancer. Prostate 1994;24:291–298.
7. Stephenson RA, Dinney CP, Gohji K, Ordonez NG, Killion JJ, Fidler IJ. Metastatic model for human prostate cancer using orthotopic implantation in nude mice. J Natl Cancer Inst 1992;84:951–957.
8. Waters DJ, Sakr WA, Hayden DW, Lang CM, McKinney L, Murphy GP, Radinsky R, Ramoner R, Richardson RC, Tindall DJ. Workgroup 4: Spontaneous prostate carcinoma in dogs and nonhuman primates. Prostate 1998;36:64–67.
9. Hall SJ, Thompson TC. Spontaneous but not experimental metastatic activities differentiate primary tumor-derived vs.

metastasis-derived mouse prostate cancer cell lines. Clin Exp Metastasis 1997;15:630–638.

10. Hall SJ, Mutchnik SE, Chen SH, Woo SL, Thompson TC. Adenovirus-mediated herpes simplex virus thymidine kinase gene and ganciclovir therapy leads to systemic activity against spontaneous and induced metastasis in an orthotopic mouse model of prostate cancer. Int J Cancer 1997;70:183–187.
11. Hall SJ, Mutchnik SE, Yang G, Timme TL, Nasu Y, Bangma CH, Woo SL, Shaker M, Thompson TC. Cooperative therapeutic effects of androgen ablation and adenovirus-mediated herpes simplex virus thymidine kinase gene and ganciclovir therapy in experimental prostate cancer. Cancer Gene Ther 1999;6:54–63.
12. Nasu Y, Bangma CH, Hull GW, Lee HM, Hu J, Wang J, McCurdy MA, Shimura S, Yang G, Timme TL, Thompson TC. Adenovirus-mediated interleukin-12 gene therapy for prostate cancer: Suppression of orthotopic tumor growth and pre-established lung metastases in an orthotopic model. Gene Ther 1999;6:338–349.
13. Nasu Y, Timme TL, Yang G, Bangma CH, Li L, Ren C, Park SH, DeLeon M, Wang J, Thompson TC. Suppression of caveolin expression induces androgen sensitivity in metastatic androgen-insensitive mouse prostate cancer cells. Nat Med 1998;4: 1062–1064.
14. Liu JB, Goldberg BB. Endoluminal vascular and nonvascular sonography: past, present, and future. AJR Am J Roentgenol 1995;165:765–774.
15. Hünerbein M, Ghadimi BM, Haensch W, Schlag PM. Transendoscopic ultrasound of esophageal and gastric cancer using miniaturized ultrasound catheter probes. Gastrointest Endosc 1998;48:371–375.
16. Bagley DH, Liu JB, Goldberg BB. Use of endoluminal ultrasound of the ureter. Semin Urol 1992;10:194–198.
17. Liu JB, Bagley DH, Conlin MJ, Merton DA, Alexander AA, Goldberg BB. Endoluminal sonographic evaluation of ureteral and renal pelvic neoplasms. J Ultrasound Med 1997;16:515–521.
18. Thompson TC, Southgate J, Kitchener G, Land H. Multistage carcinogenesis induced by ras and myc oncogenes in a reconstituted organ. Cell 1989;56:917–930.
19. Janik P, Briand P, Hartmann NR. The effect of estrone-progesterone treatment on cell proliferation kinetics of hormone-dependent GR mouse mammary tumors. Cancer Res 1975;35: 3698–3704.
20. Mazurchuk R, Glaves D, Raghavan D. Magnetic resonance imaging of response to chemotherapy in orthotopic xenografts of human bladder cancer. Clin Cancer Res 1997;3:1635–1641.
21. Chin J, Kadhim S, Garcia B, Kim YS, Karlik S. Magnetic resonance imaging for detecting and treatment monitoring of orthotopic murine bladder tumor implants. J Urol 1991;145: 1297–1301.
22. Kuriyama S, Tsujimoto T, Nakatani Y, Tsujinoue H, Yoshiji H, Mitoro A, Yamazaki M, Okuda H, Toyokawa Y, Nagao S, Nishiwaki I, Fukui H. Sonographic estimation of liver tumor development induced by oral administration of thioacetamide in rat. In Vivo 1999;13:129–134.
23. Porter KB, Tsibris JC, Porter GW, Fuchs-Young R, Nicosia SV, O'Brien WF, Spellacy WN. Effects of raloxifene in a guinea pig model for leiomyomas. Am J Obstet Gynecol 1998;179:1283–1287.
24. Kupferwasser I, Darius H, Buerke M, Rupprecht HJ, Mohr-Kahaly S, Meyer J. Transesophageal ultrasonographic imaging in rat hearts: visualization of aortic valve vegetations in non-bacterial thrombotic endocarditis. J Am Soc Echocardiogr 1998;11:201–205.
25. Alexander AA, Liu JB, McCue P, Gomella LG, Ross RP, Lattime EC. Intravesical growth of murine bladder tumors assessed by transrectal ultrasound. J Urol 1993;150:525–528.
26. Bom N, ten Hoff H, Lancee CT, Gussenhoven WJ, Bosch JG. Early and recent intraluminal ultrasound devices. Int J Card Imaging 1989;4:79–88.
27. Hawes RH. Endoscopic ultrasound. Gastrointest Endosc Clin N Am 2000;10:161–174.